

# Methane Bioattenuation and Implications for Explosion Risk Reduction along the Groundwater to Soil Surface Pathway above a Plume of Dissolved Ethanol

Jie Ma,<sup>†</sup> William G. Rixey,<sup>‡</sup> George E. DeVaul,<sup>§</sup> Brent P. Stafford,<sup>§</sup> and Pedro J. J. Alvarez<sup>\*,†</sup>

<sup>†</sup>Department of Civil and Environmental Engineering, Rice University, 6100 Main Street, Houston, Texas 77005, United States

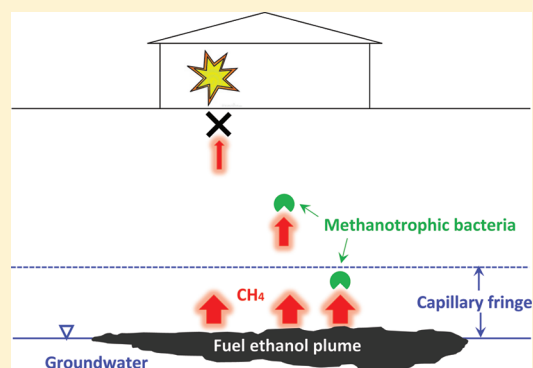
<sup>‡</sup>Department of Civil and Environmental Engineering, University of Houston, 4800 Calhoun Road, Houston, Texas 77204-4003, United States

<sup>§</sup>Shell Global Solutions (US) Inc., Westhollow Technology Center, 3333 Highway Six South, Houston, Texas 77210, United States

## Supporting Information

**ABSTRACT:** Fuel ethanol releases can stimulate methanogenesis in impacted aquifers, which could pose an explosion risk if methane migrates into enclosed spaces where ignitable conditions exist. To assess this potential risk, a flux chamber was emplaced on a pilot-scale aquifer exposed to continuous release (21 months) of an ethanol solution (10% v:v) that was introduced 22.5 cm below the water table. Despite methane concentrations within the ethanol plume reaching saturated levels (20–23 mg/L), the maximum methane concentration reaching the chamber (21 ppm<sub>v</sub>) was far below the lower explosion limit in air (50,000 ppm<sub>v</sub>). The low concentrations of methane observed in the chamber are attributed to methanotrophic activity, which was highest in the capillary fringe. This was indicated by methane degradation assays in microcosms prepared with soil samples from different depths, as well as by PCR measurements of *pmoA*, which is a widely used functional gene biomarker for methanotrophs.

Simulations with the analytical vapor intrusion model “Bio vapor” corroborated the low explosion risk associated with ethanol fuel releases under more generic conditions. Model simulations also indicated that depending on site-specific conditions, methane oxidation in the unsaturated zone could deplete the available oxygen and hinder aerobic benzene biodegradation, thus increasing benzene vapor intrusion potential. Overall, this study shows the importance of methanotrophic activity near the water table to attenuate methane generated from dissolved ethanol plumes and reduce its potential to migrate and accumulate at the surface.



## INTRODUCTION

The growing use of ethanol as transportation fuel increases the potential for ethanol-blend releases that impact groundwater and stimulate methanogenesis.<sup>1</sup> Under ignitable conditions, methane can pose an explosion risk when it accumulates in air at 50,000 to 150,000 ppm,<sup>2</sup> and ignitions have been reported at landfill sites.<sup>3,4</sup> Thus, it is important to evaluate the potential for ethanol-derived methane to migrate from impacted aquifers up into enclosed spaces and cause an explosion risk.

Several recent studies have reported relatively high methane concentrations in groundwater (23 to 47 mg/L)<sup>1,5</sup> and subsurface deep soil gas (68% v:v)<sup>6</sup> at sites impacted by fuel ethanol releases. Whereas these studies contribute to the understanding of potential methane intrusion pathways, a comprehensive assessment of the associated explosion risk needs to consider multiple processes that affect the rate and extent of methane accumulation in buildings overlying contaminated groundwater, such as phase partitioning, diffusion and advection, biodegradation, attenuation across building foundations, building ventilation, and indoor mixing.<sup>7,8</sup> In particular, there is a need for studies that quantify methane

accumulation in overlying enclosed spaces and to assess the potential for bioattenuation by methanotrophic bacteria along the groundwater to ground surface pathway. Methanotrophs are widely distributed in the environment,<sup>9</sup> but their vertical distribution and activity have not been investigated in ethanol-impacted aquifer systems.

A general assessment of explosion risks associated with ethanol blend releases would benefit from the use of vapor intrusion models that enable simulations of the fate and transport of methane under multiple scenarios. Many vapor intrusion models have been developed.<sup>10–16</sup> However, to our knowledge, such models have not been used to assess the explosion risk of methane generated from fuel ethanol spills.

Another important knowledge gap is the effect that the generated methane has on the fate and transport of benzene vapors through the unsaturated zone. Previous research on

Received: February 21, 2012

Revised: April 24, 2012

Accepted: April 25, 2012

Published: May 8, 2012

benzene vapor intrusion focused on the fate and transport of benzene alone and showed that aerobic biodegradation can significantly attenuate benzene flux and reduce its vapor intrusion potential.<sup>17–21</sup> However, the effect of methane on the biodegradation of benzene vapors is not fully understood. Aerobic biodegradation of methane or other labile compounds consumes oxygen that would otherwise be available for benzene biodegradation. Since high concentrations of benzene and methane can coexist in the vicinity of the source zone,<sup>5,22</sup> it is important to investigate whether aerobic benzene degradation in the vadose zone would be inhibited by competition for oxygen by methanotrophs, thus increasing benzene vapor intrusion.

This study addresses 1) the explosion risk associated with methanogenesis in a pilot-scale aquifer system impacted by a continuous release of fuel ethanol into groundwater; 2) the vertical distribution and effect of methanotrophs on the upward migration and fate of methane; and 3) the potential effect of oxygen consumption by methanotrophs on the benzene vapor intrusion pathway. A surface flux chamber was used to assess methane accumulation above the soil surface. Methanotrophic activity was investigated using microcosms prepared with soil samples from different depths, as well as corresponding qPCR measurements of a methanotroph functional gene (*pmoA*). The vapor intrusion model “Biovapor” was also used to assess the methane explosion risk and simulate the effect of oxygen consumption by methanotrophs on benzene vapor intrusion under differing site conditions.

## MATERIALS AND METHODS

**Pilot-Scale Aquifer System.** A pilot-scale aquifer consisting of an 8 m<sup>3</sup> (3.7 m × 1.8 m × 1.2 m) continuous-flow tank packed with fine grain sand was used for this study (Figure 1).

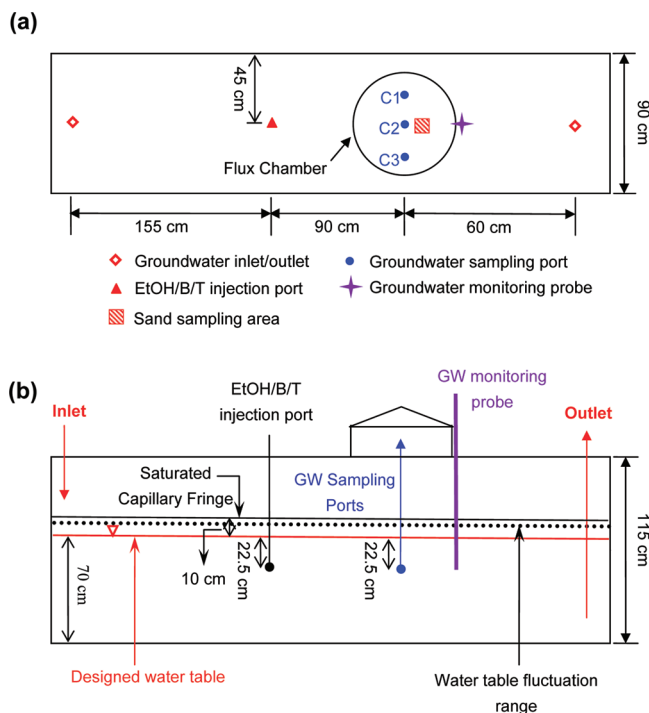


**Figure 1.** Plan view (a) and profile view (b) of the pilot-scale aquifer system. The ethanol blend was injected through a stainless steel tube (inner diameter: 5 mm) at 22.5 cm below the water table.

Details of tank construction, gravity-fed hydraulics, porous media, and packing methods were previously reported.<sup>23,24</sup> Tap water amended with 10% (v/v) ethanol, 50 mg/L benzene, 50 mg/L toluene (E/B/T), and 24,000 mg/L of sodium bromide was continuously injected into the channel through a stainless steel tube (inner diameter: 5 mm) at 22.5 cm below the water table (67.5 cm below ground surface (BGS)) at a rate of 0.4 L/day. NaBr was added as a conservative tracer and to maintain a solution density to reach neutral buoyancy with the flowing groundwater.<sup>25</sup> Tap water was added at 170 L/day (average seepage velocity of 2.5 ft/day) to obtain a water table elevation of about 70 cm from the bottom of the tank. The total aquifer thickness was 115 cm, and the depth of the water table was 45 cm BGS. The top 5 cm of the soil was air-dried as previously described.<sup>24</sup> A 10-cm layer above the water table was saturated with groundwater due to capillary action. Because of the small variation in groundwater flow rate, the depths of the water table (as well as the upper boundary of saturated capillary fringe) varied between 35 and 45 cm BGS. All groundwater sampling ports (C1, C2, C3) were placed at the same depth as the injection point (67.5 cm BGS). A stainless steel dome-shaped flux chamber was emplaced to measure methane accumulation at the surface (Figure S1). Details regarding the flux chamber are given in the Supporting Information (SI). Groundwater geochemical characteristics including temperature and dissolved oxygen were monitored by a YSI 600XLM groundwater monitoring probe (YSI Inc., Yellow Springs, Ohio) (Figure 1).

**Sampling and Analysis Methods for CH<sub>4</sub> and O<sub>2</sub>.** To measure CH<sub>4</sub> accumulation in the flux chamber, 30 mL headspace gas samples were collected from the top sampling port using VICI Series A-2 Precision Sampling Syringes (VICI Instruments Co. Inc., Baton Rouge, LA). Gas samples were immediately transferred to SKC single polypropylene fitted bags (SKC Inc., Eighty Four, PA) and taken to the lab for CH<sub>4</sub> analysis. To measure the vertical concentration profiles of CH<sub>4</sub> and O<sub>2</sub> in the unsaturated zone, 100 μL of soil pore gas samples at different depths (5, 10, 15, 20, 25, and 30 cm BGS) were collected in six replicates using VICI Series A-2 Precision Sampling Syringes (VICI Instruments Co. Inc., Baton Rouge, LA) and analyzed immediately in the lab on July 4 and 5, 2011. CH<sub>4</sub> was analyzed as described previously,<sup>26</sup> using a HP5890 GC-FID (Agilent Technologies Inc., Santa Clara, CA) equipped with a packed column (1% SP-1000 on Carbowack-B (60/80) mesh; Supelco, Bellefonte, PA). O<sub>2</sub> was analyzed with an Agilent 7890 GC-TCD equipped with a HP-PLOT MoleSieve column (Agilent Technologies Inc., Santa Clara, CA).

**Assessment of Methane Oxidation Activity at Different Depths.** To assess the vertical distribution of the methane oxidation activity and the spatial variability of the concentration of a representative methanotrophic functional gene (*pmoA*), soil samples were collected from different depths in the pilot-scale aquifer (5 to 10 cm BGS and 15 to 20 cm BGS for the unsaturated zone; 30 to 40 cm BGS for the saturated capillary fringe; 40 to 50 cm BGS cm for the region across the water table, and 60 to 70 cm BGS for the anaerobic saturated zone near the centerline of ethanol plume). Soil cores above the water table (5 to 10 cm BGS, 15 to 20 cm BGS, and 30 to 40 cm BGS) were collected using a PVC pipe (1.25 cm diameter). The sampling pipe was hammered down to the desired depth. Then the top of the pipe was sealed with duct tape, and the pipe was extracted by hand. Each depth was sampled 5 times to get enough soil (>50 g). The five sampling locations were

within a 10 cm × 10 cm area (Figure 1). Soil samples in the saturated zone (40 to 50 cm BGS and 60 to 70 cm BGS) were collected using a Sand Sludge Sediment Sampling Probe (diameter 2.5 cm) (AMS Inc., American Falls, ID).

Microcosms were prepared in triplicate to measure methane biodegradation activity in soil samples. The soil samples (15 g) were mixed with 10 mL of sterile H<sub>2</sub>O and placed in sterile 125-mL serum bottles before sealing with gastight butyl rubber stoppers and aluminum crimp caps. For sterilized soil controls, 15 g of soil was placed into a 125-mL serum bottle and autoclaved at 121 °C for 30 min. Each bottle was then supplemented with 1 mL of methane (approximately 10<sup>4</sup> ppm<sub>v</sub>) and incubated in a rotary shaker at 150 rpm and 37 °C. This temperature is higher than the average temperature in the tank and would likely be only achieved sporadically during the summer. However, it is close to the optimum temperature for many methanotrophs<sup>27–29</sup> and was selected to accelerate the determination of the relative distribution of methanotrophic activity along the depth of the vadose zone. Headspace methane was measured as described above. From the methane depletion data, linear regressions were calculated, and biodegradation rates were determined as the slope of the regression.

**qPCR Assays for *pmoA* Gene.** The first step of methane oxidation is catalyzed by methane monooxygenase (MMO), which hydroxylates the molecule. There are two types of MMO: a particulate membrane-bound form (pMMO) and a soluble form (mMMO). The latter has been found only in some methanotrophs, while pMMO exists in almost all isolated methanotrophs except for *Methylocella* species.<sup>30</sup> The *pmoA* gene encodes the  $\alpha$ -subunit of pMMO and has been shown to be highly conserved. It is often used as a biomarker for methanotrophs.<sup>31,32</sup>

Quantitative PCR (qPCR) analyses were performed for the same soil samples used in the microcosms, as described elsewhere.<sup>31</sup> Five different assays (MBAC, MCOC, MCAP, FOREST, and TYPEII) were performed to detect different phylogenetic subgroups of methanotrophs that contain *pmoA*.<sup>31</sup> DNA was extracted in four replicates from 0.25 g of soil using PowerSoil DNA Kit (MOBIO Inc., Carlsbad, CA). Details about the qPCR method are given in the Supporting Information (SI), including primer sets and annealing temperatures (Table S1).

**Model Simulation.** “Bio vapor” is an analytic vapor intrusion model which is based on the widely used Johnson and Ettinger’s model,<sup>10</sup> and it additionally includes oxygen-limited biodegradation.<sup>11,33</sup> “Bio vapor” incorporates a steady-state vapor source, diffusion-dominated soil vapor migration in a homogeneous soil layer, and mixing within a building enclosure. An illustrative conceptual model assumed in “Bio vapor” is presented in Figure S2. The soil is divided into a shallow aerobic layer including biodegradation and a deeper anaerobic layer in which biodegradation is omitted. Oxygen demand is attributed to a sum of baseline respiration of soil organic matter and biodegradation of multiple chemicals assuming first-order degradation rates. The model is solved by iteratively varying the aerobic depth to match oxygen demand to oxygen supply. “Bio vapor” was used to calculate the methane indoor concentrations under different scenarios (e.g., different source concentrations, source depths, with and without biodegradation) using parameters listed in Table S2. “Bio vapor” was also used to simulate benzene vapor intrusion under different conditions, using parameters listed in Table S3.

Model input parameters were based on values that are commonly used for risk assessments.<sup>33</sup>

## RESULTS AND DISCUSSION

**Methane Accumulation in the Flux Chamber.** Methane emissions from the soil surface were measured using a static flux chamber of internal volume ( $V$ ) = 8.5 × 10<sup>4</sup> cm<sup>3</sup> and surface area ( $A$ ) = 2.8 × 10<sup>3</sup> cm<sup>2</sup>. Four measurement events were made in different seasons (Figure 2). Methane

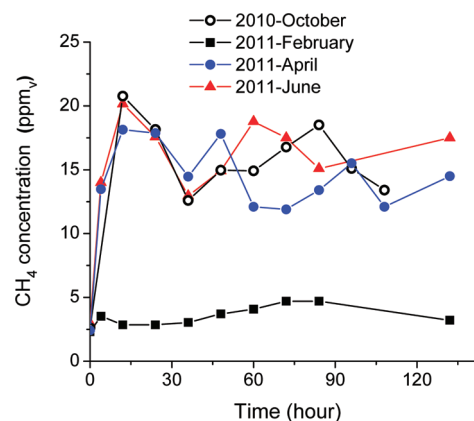


**Figure 2.** Methane accumulations inside the flux chamber in different seasons.

concentrations inside the chamber increased exponentially ( $k = 0.26 \text{ h}^{-1}$ ) and reached an asymptotic concentration 30 to 80 h after the chamber was emplaced. With a presumed constant emission flux of methane from the soil surface (during the sampling period) and low methane concentrations in ambient air, this implied an effective passive air flow rate ( $Q$ ) through the chamber of  $Q = V \cdot k = 2.2 \times 10^4 \text{ cm}^3/\text{h}$ . Thus, the surface methane emission flux ( $J$ ) was estimated as  $J = Q \cdot C_a/A$  (Table 1), where  $C_a$  is the average asymptotic chamber concentration.

**Table 1.** Measured CH<sub>4</sub> Concentration and Calculated Surface Flux

sampling date	average asymptotic CH <sub>4</sub> concentration in the flux chamber <sup>a</sup> ( $C_a$ )		calculated surface emission flux ( $J$ )
	ppm <sub>v</sub>	mg/cm <sup>3</sup>	
October 2010	15.5 ± 2.1	1.0 ± 0.1 × 10 <sup>-5</sup>	8.0 ± 1.1 × 10 <sup>-5</sup>
February 2011	3.7 ± 0.8	2.4 ± 0.5 × 10 <sup>-6</sup>	1.9 ± 0.4 × 10 <sup>-5</sup>
April 2011	14.8 ± 2.5	9.7 ± 1.6 × 10 <sup>-6</sup>	7.7 ± 1.3 × 10 <sup>-5</sup>
June 2011	16.8 ± 2.3	1.1 ± 0.1 × 10 <sup>-5</sup>	8.7 ± 1.2 × 10 <sup>-5</sup>

<sup>a</sup>Average CH<sub>4</sub> concentrations ( $C_a$ ) and standard deviations were calculated from 8 to 10 data points after reaching pseudosteady state (Figure 2).

The seasonal variation in  $J$  ( $1.9 \pm 4.0 \times 10^{-5}$  to  $8.7 \pm 1.2 \times 10^{-5} \text{ mg/cm}^2\text{-h}$ ) reflects differences in methane generation rates at different groundwater temperatures (February: 7 °C, April: 23 °C, June: 28 °C, October: 26 °C),<sup>25</sup> with higher values observed during summer months when groundwater was saturated with methane (Table S4). The solubility of methane is 21.4 mg/L at 28 °C.<sup>34</sup> The maximum concentration of methane in the headspace of the flux chamber was 21 ppm<sub>v</sub>, a value far below the methane vapor concentrations in

equilibrium with saturated groundwater (i.e.,  $10^6$  ppm<sub>v</sub>), and also far below the lower explosion limit (LEL, 50,000 ppm<sub>v</sub>) for methane in ambient air.<sup>2</sup>

**Aerobic Biodegradation of Methane in the Pilot-Scale Aquifer.** The vertical methane concentration profile shows that more than 99% of the methane was attenuated before reaching the unsaturated zone (30 cm BGS; Figure 3). The average

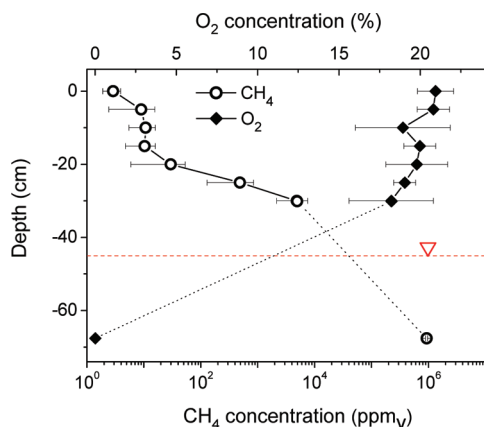


**Figure 3.** Vertical concentration profiles of methane and oxygen in the soil gas near the groundwater sampling port C2 (Figure 1) measured on July 4 and 5, 2011. Methane concentration at 67.5 cm BGS was calculated based on the measured groundwater concentration using Henry's law. The dissolved oxygen concentration at 67.5 cm BGS was measured by the groundwater geochemical monitoring probe (Figure 1).

methane concentration at 30 cm BGS was  $4.9 \times 10^3 \pm 2.7 \times 10^3$  ppm<sub>v</sub>, which is only 0.5% of the equilibrium methane concentration for the saturated groundwater ( $10^6$  ppm<sub>v</sub>). The low methane concentrations in the unsaturated zone represent a low biochemical oxygen demand and no significant oxygen depletion occurred in that zone (Figure 3). The relative contribution of biodegradation to methane attenuation in the unsaturated zone (15 to 30 cm BGS) likely exceeds 99%, as estimated by a one-dimensional steady-state diffusion model with first-order reaction (see the SI).

Microcosm assays and *pmoA* analysis (Figure 4) show that the saturated capillary fringe (30 to 40 cm BGS) exhibited the highest methanotrophic activity ( $0.51 \pm 0.028$   $\mu\text{g CH}_4/\text{h/g soil}$  and  $2.2 \times 10^7 \pm 4.8 \times 10^6$  *pmoA* gene copies/g soil). Furthermore, methane degradation rate and *pmoA* copy numbers were significantly correlated ( $p < 0.05$ , Figure S3), corroborating the usefulness of this biomarker to assess methane bioattenuation potential. Apparently, the coexistence of relatively high fluxes and resulting high concentrations of methane ( $>2.9 \times 10^3$  ppm<sub>v</sub>) and oxygen (21% v:v at 30 BGS) in the capillary fringe favored the proliferation and activity of methanotrophs. Furthermore, the soil pores in the capillary fringe were saturated with water, and the molecular diffusion coefficient of methane in air ( $2.1 \times 10^{-1}$  cm<sup>2</sup>/s) is 5600 times higher than that in water ( $3.8 \times 10^{-5}$  cm<sup>2</sup>/s).<sup>35</sup> Therefore, the capillary fringe had a much smaller effective diffusion coefficient than the overlying unsaturated zone, which was conducive to longer retention time for both methane and oxygen. This likely also contributed to the proliferation and relatively high activity of methanotrophs in that layer. Relatively high aerobic biodegradation activity of hydrocarbon vapors in the capillary fringe has also been reported.<sup>36</sup> In addition to biodegradation,

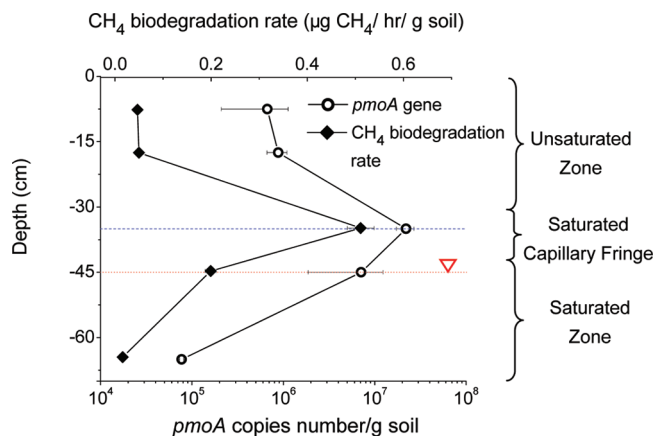


**Figure 4.** Vertical distribution of *pmoA* gene concentration and methane biodegradation rate in the pilot-scale aquifer. Degradation rates and *pmoA* copy numbers were significantly correlated ( $r^2 = 0.977$ ,  $p < 0.05$ , Figure S3). The designed water table was at 45 cm BGS (red dotted line). A 10 cm layer above the water table was usually saturated with groundwater due to capillary action (blue dash line). Due to the fluctuation of the water table, the actual upper boundaries of saturated zone and capillary fringe were often several centimeters higher than the designed levels.

the slower diffusion of methane through the capillary fringe also decreased the flux and contributed to the attenuation of methane concentrations reaching the surface.

The absence of lag phases during the biodegradation assays (Figure S4) indicates that the methanotrophs were already adapted. The maximum methane biodegradation rate ( $0.51 \pm 0.028$   $\mu\text{g CH}_4/\text{h/g soil}$ , in capillary fringe) was comparable to some reported biodegradation rates for landfill cover soils (e.g.,  $0.65$   $\mu\text{g CH}_4/\text{h/g soil}$ <sup>37</sup> and  $0.75$   $\mu\text{g CH}_4/\text{h/g soil}$ <sup>38</sup>), although much higher biodegradation rates have been reported for similar systems (e.g.,  $112$   $\mu\text{g CH}_4/\text{h/g soil}$ <sup>39</sup>).

Five different qPCR assays were conducted to assess the presence of different phylogenetic subgroups of methanotrophs harboring the *pmoA* gene. Only the MBAC assay yielded detectable PCR amplification, indicating that the dominant methanotrophs in this pilot aquifer belong to genus *Methylobacter* or *Methylosarcina*.<sup>31</sup>

Note that the release under consideration was introduced below the water table and did not generate residual ethanol in the vadose zone, as may be the case for releases above groundwater where ethanol may be trapped or remain coated on soil particles for an extended time.<sup>40,41</sup> Such residual ethanol can serve as an additional source of methane in the unsaturated zone, and the resulting localized anaerobic conditions would hinder aerobic methanotrophic activity. Thus, although this study demonstrates the importance of methane bioattenuation along the groundwater to soil surface pathway, the rate and extent of methane reaching the surface will likely be system-specific.

**Methane Accumulation Simulations.** "Biovapor" simulations corroborate the nonexistence of explosion risk in overlying confined spaces associated with diffusion-driven methane migration under more generic conditions. Simulated methane indoor concentrations increase as the source concentration increases and the source depth decreases (Figure 5). However, even under the worst-case scenario examined here (i.e., high methane source concentration, shallow source depth and no biodegradation), the simulated methane indoor

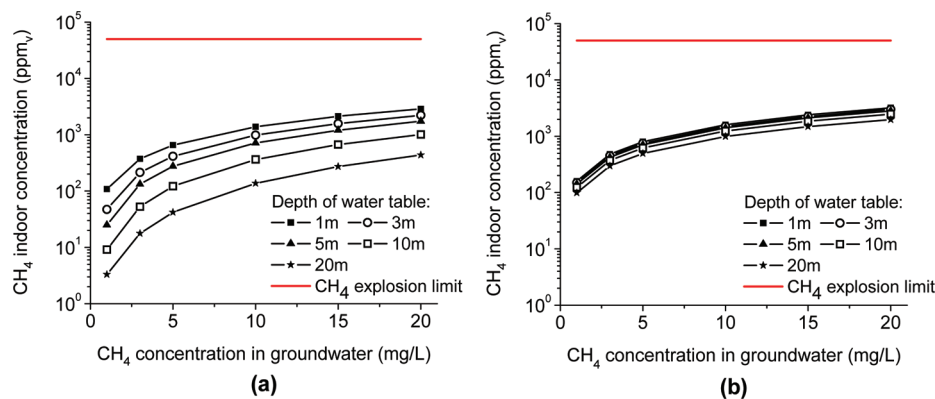


**Figure 5.** Simulated methane indoor concentrations (a) with and (b) without methane biodegradation under different source concentrations and depths to water table. Simulation parameters are given in Table S2.

concentration is still much lower than the lower explosion limit for methane (50,000 ppm<sub>v</sub>). Model simulations also corroborate that aerobic biodegradation significantly reduces the methane flux into the enclosure ( $J_f$  in Figure S2) by 78% to 99%, depending on the source concentration and depth. If the methane source concentration is high (e.g., 20 mg/L in groundwater) and the source is shallow (e.g., 1 m), methane oxidation would be limited by oxygen availability, but biodegradation still decreases  $J_f$  by 78%. If the methane source concentration is low (e.g., 1 mg/L) and the source is deep (e.g., 20 m), more methane would be biodegraded (99% of  $J_f$ ) and the simulated concentrations with biodegradation would be much lower (e.g., 3%) than those simulated without biodegradation.

“Bio vapor” assumes that diffusion is the only vapor transportation pathway in the vadose zone.<sup>33</sup> This assumption is appropriate for many contaminated sites.<sup>10,42</sup> However, we cannot exclude the possibility that in some scenarios methanogenesis could be strong enough to increase the pore pressure near the source and produce significant vertical advective flow in the vadose zone.<sup>43,44</sup> In the pilot-scale aquifer system, the groundwater residence time (from injection point to downstream sampling port) was approximately one day. The total conversion of ethanol along this path ranged from approximately 10% in the winter to >50% in the summer. However, we could not discern the fraction of the degraded ethanol that was converted to methane vs other products, and what fraction of this methane was transported vertically to the surface. It is possible that a longer groundwater residence time could yield more conversion to methane with potentially higher methane concentrations and mass fluxes in the unsaturated zone. Thus, further research is needed to address the possible advective contribution to methane fluxes in the vadose zone overlying ethanol blend releases.

**Impacts of Methane Oxidation on Benzene Vapor Intrusion.** Experimental conditions (e.g., shallow water table with open surface without overlying structures, sandy porous medium that facilitate aeration, relatively low biomass concentration in the unsaturated zone, and high methanotrophic activity in the capillary zone) precluded significant oxygen consumption in the unsaturated zone of this pilot aquifer system. However, oxygen depletion has been reported in the vadose zone of many fuel contaminated sites<sup>45–47</sup> and landfill cover soil.<sup>48</sup> Therefore, simulations were conducted using “Bio vapor” to investigate how oxygen consumption by methanotrophs in the vadose zone might affect hydrocarbon

vapor intrusion pathways under broader release scenarios. Benzene, which is commonly the selected risk driver in vapor intrusion risk assessments for fuel impacted sites,<sup>49</sup> was chosen in this modeling effort.

Model simulations indicate that under more generic conditions examined here, methane oxidation could deplete oxygen that would otherwise be consumed in benzene degradation, thereby increasing potential benzene vapor intrusion. When methane is absent in the groundwater, extensive aerobic biodegradation of benzene vapors occurs in the vadose zone and the simulated benzene indoor concentration is more than 6 orders of magnitude lower than the EPA screening level (0.31  $\mu\text{g}/\text{m}^3$ ) (Figure 6). Benzene

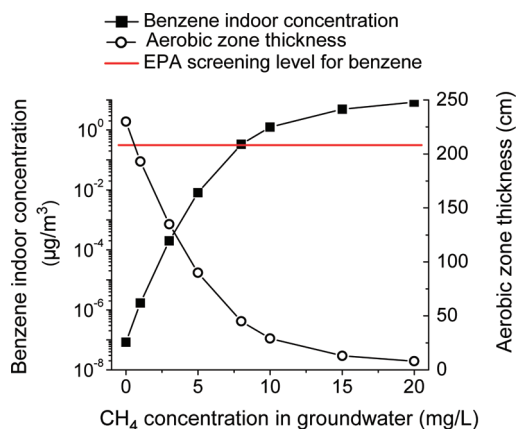


**Figure 6.** Simulated benzene indoor concentrations and the aerobic zone thickness for different methane groundwater concentrations. Simulation parameters are given in Table S3.

indoor concentrations increase with methane groundwater concentrations. If the methane groundwater concentration reaches 20 mg/L, the benzene indoor concentration reaches 8.5  $\mu\text{g}/\text{m}^3$ , which is 27 times higher than the EPA screening level. Competition for oxygen is the major reason that benzene vapor intrusion is enhanced. Oxygen consumption and aerobic zone thickness were calculated by “Bio vapor”. The aerobic zone is conservatively defined as the soil region with oxygen concentration higher than 1% (v:v), which is conservatively assumed to be the minimum oxygen level under which aerobic biodegradation can occur.<sup>33</sup> As methane groundwater concentrations increase, more oxygen is consumed by methane oxidation, and the aerobic zone thickness decreases sharply

(Figure 6). We simulated a worse-case scenario evaluated here (high benzene groundwater concentration (10 mg/L), high methane groundwater concentration (20 mg/L), and low depth to the water table (3 m)). The simulated benzene indoor concentration was  $1.6 \times 10^3 \mu\text{g}/\text{m}^3$ , which is 5,300 times higher than the EPA screening level. However, for the same conditions without methane, the simulated benzene indoor concentration was only  $1.2 \times 10^{-2} \mu\text{g}/\text{m}^3$ , which is significantly lower than the EPA screening level. Methanotrophic activity increases the simulated benzene flux into the enclosure by  $1.3 \times 10^5$  times from  $2.2 \times 10^{-4}$  to  $30 \mu\text{g}/\text{s}$ .

Overall, whereas fuel ethanol releases can stimulate significant methanogenic activity in groundwater under the conditions examined here, both model simulations and flux chamber measurements indicate that methane is unlikely to build up to explosive levels in overlying confined spaces. Methanotrophs can significantly attenuate methane migration through the vadose zone, particularly in the capillary zone where slower diffusion of methane enhances retention time and facilitates adequate moisture and oxygen availability to favor methanotrophic activity. Nevertheless, aerobic biodegradation of methane may have a negative effect. Depending on the release scenario, methanotrophs could deplete the available oxygen and reduce the near-source attenuation for other volatile compounds such as benzene, increasing their vapor intrusion potential.

## ■ ASSOCIATED CONTENT

### 📄 Supporting Information

Details on the flux chamber, qPCR method, "Bio vapor" model, model simulation inputs, measured methane groundwater concentration data, methane biodegradation data measured in microcosms, the correlation between methane degradation rate and *pmoA* gene abundance, and the calculation process to estimate the contribution of methanotrophic activity in methane attenuation. This material is available free of charge via the Internet at <http://pubs.acs.org>.

## ■ AUTHOR INFORMATION

### Corresponding Author

\*Phone: 713-348-5903. Fax: 713-348-5203. E-mail: [alvarez@rice.edu](mailto:alvarez@rice.edu)

### Notes

The authors declare no competing financial interest.

## ■ ACKNOWLEDGMENTS

This work was funded by the American Petroleum Institute. Jie Ma also received partial support from a scholarship from the China Scholarship Council. We thank Yi Zhang for his assistance in tank preparation and Dr. Hong Luo for her advice on model simulations.

## ■ REFERENCES

- Freitas, J. G.; Fletcher, B.; Aravena, R.; Barker, J. F. Methane production and isotopic fingerprinting in ethanol fuel contaminated sites. *Ground Water* **2010**, *48* (6), 844–857.
- Bjerketvedt, D.; Bakke, J. R.; van Wingerden, K. Gas explosion handbook. *J. Hazard. Mater.* **1997**, *52* (1), 1–150.
- Williams, G. M.; Aitkenhead, N. Lessons from Loscoe—the uncontrolled migration of landfill gas. *Q. J. Eng. Geol.* **1991**, *24* (2), 191–207.

- Kjeldsen, P. Landfill gas migration in soil. In *Landfilling of Waste: Biogas*; Christensen, T. H., Cossu, R., Stegmann, R., Eds.; E & FN Spon: London, UK, 1996.

- Spalding, R. F.; Toso, M. A.; Exner, M. E.; Hattan, G.; Higgins, T. M.; Sekely, A. C.; Jensen, S. D. Long-term groundwater monitoring results at large, sudden denatured ethanol releases. *Ground Water Monit. Rem.* **2011**, *31* (3), 69–81.

- Jewell, K. P.; Wilson, J. T. A new screening method for methane in soil gas using existing groundwater monitoring wells. *Ground Water Monit. Rem.* **2011**, *31* (3), 82–94.

- Rivett, M. O.; Wealthall, G. P.; Dearden, R. A.; McAlary, T. A. Review of unsaturated-zone transport and attenuation of volatile organic compound (VOC) plumes leached from shallow source zones. *J. Contam. Hydrol.* **2011**, *123* (3–4), 130–156.

- Patterson, B. M.; Davis, G. B. Quantification of vapor intrusion pathways into a slab-on-ground building under varying environmental conditions. *Environ. Sci. Technol.* **2009**, *43* (3), 650–656.

- Hanson, R. S.; Hanson, T. E. Methanotrophic bacteria. *Microbiol. Rev.* **1996**, *60* (2), 439–471.

- Johnson, P. C.; Ettinger, R. A. Heuristic model for predicting the intrusion rate of contaminant vapors into buildings. *Environ. Sci. Technol.* **1991**, *25* (8), 1445–1452.

- DeVaul, G. E. Indoor vapor intrusion with oxygen-limited biodegradation for a subsurface gasoline source. *Environ. Sci. Technol.* **2007**, *41* (9), 3241–3248.

- Abreu, L. D. V.; Johnson, P. C. Effect of vapor source - building separation and building construction on soil vapor intrusion as studied with a three-dimensional numerical model. *Environ. Sci. Technol.* **2005**, *39* (12), 4550–4561.

- Pennell, K. G.; Bozkurt, O.; Suuberg, E. M. Development and application of a three-dimensional finite element vapor intrusion model. *J. Air Waste Manage. Assoc.* **2009**, *59* (4), 447–460.

- Parker, J. C. Modeling volatile chemical transport, biodecay, and emission to indoor air. *Ground Water Monit. Rem.* **2003**, *23* (1), 107–120.

- Mills, W. B.; Liu, S.; Rigby, M. C.; Brenner, D. Time-variable simulation of soil vapor intrusion into a building with a combined crawl space and basement. *Environ. Sci. Technol.* **2007**, *41* (14), 4993–5001.

- Mayer, K. U.; Frind, E. O.; Blowes, D. W. Multicomponent reactive transport modeling in variably saturated porous media using a generalized formulation for kinetically controlled reactions. *Water Resour. Res.* **2002**, *38*, 9.

- Hers, I.; Atwater, J.; Li, L.; Zapf-Gilje, R. Evaluation of vadose zone biodegradation of BTX vapours. *J. Contam. Hydrol.* **2000**, *46* (3–4), 233–264.

- Abreu, L. D. V.; Johnson, P. C. Simulating the effect of aerobic biodegradation on soil vapor intrusion into buildings: Influence of degradation rate, source concentration, and depth. *Environ. Sci. Technol.* **2006**, *40* (7), 2304–2315.

- Davis, G. B.; Rayner, J. L.; Trefry, M. G.; Fisher, S. J.; Patterson, B. M. Measurement and modeling of temporal variations in hydrocarbon vapor behavior in a layered soil profile. *Vadose Zone J.* **2005**, *4* (2), 225–239.

- Davis, G. B.; Patterson, B. M.; Trefry, M. G. Evidence for instantaneous oxygen-limited biodegradation of petroleum hydrocarbon vapors in the subsurface. *Ground Water Monit. Rem.* **2009**, *29* (1), 126–137.

- Kristensen, A. H.; Poulsen, T. G.; Mortensen, L.; Moldrup, P. Variability of soil potential for biodegradation of petroleum hydrocarbons in a heterogeneous subsurface. *J. Hazard. Mater.* **2010**, *179* (1–3), 573–580.

- Corseuil, H. X.; Monier, A. L.; Fernandes, M.; Schneider, M. R.; Nunes, C. C.; do Rosario, M.; Alvarez, P. J. J. BTEX plume dynamics following an ethanol blend release: geochemical footprint and thermodynamic constraints on natural attenuation. *Environ. Sci. Technol.* **2011**, *45* (8), 3422–3429.

- Capiro, N. L.; Stafford, B. P.; Rixey, W. G.; Bedient, P. B.; Alvarez, P. J. J. Fuel-grade ethanol transport and impacts to

groundwater in a pilot-scale aquifer tank. *Water Res.* **2007**, *41* (3), 656–664.

(24) Stafford, B. P.; Capiro, N. L.; Alvarez, P. J. J.; Rixey, W. G. Pore water characteristics following a release of neat ethanol onto pre-existing NAPL. *Ground Water Monit. Rem.* **2009**, *29* (3), 93–104.

(25) Ma, J.; Xiu, Z.; Monier, A.; Mamonkina, L.; Zhang, Y.; He, Y.; Stafford, B.; Rixey, W.; Alvarez, P. Aesthetic groundwater quality impacts from a continuous pilot-scale release of an ethanol blend. *Ground Water Monit. Rem.* **2011**, *31* (3), 47–54.

(26) Capiro, N. L.; Da Silva, M. L. B.; Stafford, B. P.; Rixey, W. G.; Alvarez, P. J. J. Microbial community response to a release of neat ethanol onto residual hydrocarbons in a pilot-scale aquifer tank. *Environ. Microbiol.* **2008**, *10* (9), 2236–2244.

(27) Whalen, S. C.; Reeburgh, W. S.; Sandbeck, K. A. Rapid methane oxidation in a landfill cover soil. *Appl. Environ. Microbiol.* **1990**, *56* (11), 3405–3411.

(28) King, G. M.; Adamsen, A. P. S. Effects of temperature on methane consumption in a forest soil and in pure cultures of the methanotroph *Methylomonas rubra*. *Appl. Environ. Microbiol.* **1992**, *58* (9), 2758–2763.

(29) Mohanty, S. R.; Bodelier, P. L. E.; Conrad, R. Effect of temperature on composition of the methanotrophic community in rice field and forest soil. *FEMS Microbiol. Ecol.* **2007**, *62* (1), 24–31.

(30) Dedysh, S. N.; Liesack, W.; Khmelenina, V. N.; Suzina, N. E.; Trotsenko, Y. A.; Semrau, J. D.; Bares, A. M.; Panikov, N. S.; Tiedje, J. M. *Methylocella palustris* gen. nov., sp. nov., a new methane-oxidizing acidophilic bacterium from peat bogs, representing a novel subtype of serine-pathway methanotrophs. *Int. J. Syst. Evol. Microbiol.* **2000**, *50*, 955–969.

(31) Kolb, S.; Knief, C.; Stubner, S.; Conrad, R. Quantitative detection of methanotrophs in soil by novel pmoA-targeted real-time PCR assays. *Appl. Environ. Microbiol.* **2003**, *69* (5), 2423–2429.

(32) McDonald, I. R.; Bodrossy, L.; Chen, Y.; Murrell, J. C. Molecular ecology techniques for the study of aerobic methanotrophs. *Appl. Environ. Microbiol.* **2008**, *74* (5), 1305–1315.

(33) DeVuall, G.; McHugh, T. E.; Newberry, P. *Users Manual "BioVapor: a 1-D Vapor Intrusion Model with Oxygen-Limited Aerobic Biodegradation"*; American Petroleum Institute: Washington, DC, 2010. <http://www.api.org/Environment-Health-and-Safety/Clean-Water/Ground-Water/Vapor-Intrusion/BioVapor.aspx> (accessed July 22, 2011).

(34) Yamamoto, S.; Alcauskas, J. B.; Crozier, T. E. Solubility of methane in distilled water and seawater. *J. Chem. Eng. Data* **1976**, *21* (1), 78–80.

(35) Schwarzenbach, R. P.; Gschwend, P. M.; Imboden, D. M. *Environmental Organic Chemistry*, 2nd ed.; Wiley-Interscience: Hoboken, NJ, 2002.

(36) Lahvis, M. A.; Baehr, A. L. Estimation of rates of aerobic hydrocarbon biodegradation by simulation of gas transport in the unsaturated zone. *Water Resour. Res.* **1996**, *32* (7), 2231–2249.

(37) Jones, H. A.; Nedwell, D. B. Methane emission and methane oxidation in land-fill cover soil. *FEMS Microbiol. Ecol.* **1993**, *102* (3–4), 185–195.

(38) Schuetz, C.; Bogner, J.; Chanton, J.; Blake, D.; Morcet, M.; Kjeldsen, P. Comparative oxidation and net emissions of methane and selected non-methane organic compounds in landfill cover soils. *Environ. Sci. Technol.* **2003**, *37* (22), 5150–5158.

(39) Schuetz, C.; Mosbaek, H.; Kjeldsen, P. Attenuation of methane and volatile organic compounds in landfill soil covers. *J. Environ. Qual.* **2004**, *33* (1), 61–71.

(40) Freitas, J. G.; Barker, J. F. Oxygenated gasoline release in the unsaturated zone - Part 1: Source zone behavior. *J. Contam. Hydrol.* **2011**, *126* (3–4), 153–166.

(41) Freitas, J. G.; Doulatyari, B.; Molson, J. W.; Barker, J. F. Oxygenated gasoline release in the unsaturated zone, Part 2: Downgradient transport of ethanol and hydrocarbons. *J. Contam. Hydrol.* **2011**, *125* (1–4), 70–85.

(42) McHugh, T. E.; McAlary, T. Important physical processes for vapor intrusion: a literature review. In *Proceedings of AWMA Vapor Intrusion Conference*, San Diego, CA, 2009.

(43) Amos, R. T.; Mayer, K. U. Investigating ebullition in a sand column using dissolved gas analysis and reactive transport modeling. *Environ. Sci. Technol.* **2006**, *40* (17), 5361–5367.

(44) Amos, R. T.; Mayer, K. U. Investigating the role of gas bubble formation and entrapment in contaminated aquifers: Reactive transport modelling. *J. Contam. Hydrol.* **2006**, *87* (1–2), 123–154.

(45) Lundegard, P. D.; Johnson, P. C.; Dahlen, P. Oxygen transport from the atmosphere to soil gas beneath a slab-on-grade foundation overlying petroleum-impacted soil. *Environ. Sci. Technol.* **2008**, *42* (15), 5534–5540.

(46) Lundegard, P. D.; Johnson, P. C. Source zone natural attenuation at petroleum hydrocarbon spill sites - II: Application to a former oil field. *Ground Water Monit. Rem.* **2006**, *26* (4), 93–106.

(47) Molins, S.; Mayer, K. U.; Amos, R. T.; Bekins, B. A. Vadose zone attenuation of organic compounds at a crude oil spill site - Interactions between biogeochemical reactions and multicomponent gas transport. *J. Contam. Hydrol.* **2010**, *112* (1–4), 15–29.

(48) Molins, S.; Mayer, K. U.; Scheutz, C.; Kjeldsen, P. Transport and reaction processes affecting the attenuation of landfill gas in cover soils. *J. Environ. Qual.* **2008**, *37* (2), 459–468.

(49) U.S.EPA *Draft guidance for evaluating the vapor intrusion to indoor air pathway from groundwater and soils (subsurface vapor intrusion guidance)*; Office of Solid Waste and Emergency: Washington, DC, 2002. <http://www.epa.gov/correctiveaction/eis/vapor/guidance.pdf> (accessed April 3, 2011).